Robust Predictive Current Control of Permanent-Magnet Synchronous Motors With Newly Designed Cost Function

Xicai Liu, Libing Zhou, *Member, IEEE*, Jin Wang, *Member, IEEE*, Xiaonan Gao, *Student Member, IEEE*, Zhixiong Li, *Student Member, IEEE*, and Zhiwei Zhang, *Member, IEEE*

***Abstract*—In model predictive control, mathematical model of the system is used to predict the value of state variables. Control performances of model predictive control suffer from parameter mismatches and model uncertainties. Steady-state errors will exist due to inaccurate predictions. This article presents a simple predictive current control strategy for robustness improvement of finite control set-model predictive control, with which steady-state errors under parameter mismatches can be eliminated. Neither disturbance observer nor explicit solution of compensation voltage is needed in the proposed control strategy. A cost function is newly designed, which is in proportional-integral form. Moreover, the integral action is only activated in a predefined range, which facilitates the design of the integral coefficients. The accumulated error is not simply included but weighted with the sampling time. In this way, a careful selection of the number of integral terms to be included in the cost function is not required. Experimental results demonstrate superior robustness of the proposed current control strategy to that of conventional predictive current control against parameter uncertainties.**

***Index Terms*—Finite control set-model predictive control (FCS-MPC), parameter mismatch, permanent-magnet synchronous motor (PMSM), robustness.**

I. Introduction

RECENTLY, model predictive control (MPC), which can be separated into continuous control set-MPC (CCS-MPC) and finite control set-MPC (FCS-MPC), has been increasingly investigated for the control of electrical drives and power electronics due to its intuitive principle, fast transient performance, straightforward control of multiple variables while considering nonlinearities and constraints of the system [1]–[3].

The applications of FCS-MPC on electrical drives take advantages of the discrete nature of power converters. State variables are predicted with the discrete system model for finite number of switching vectors. The switching vector which minimizes the cost function is applied to the power converter. Applications of FCS-MPC to electrical drives range from conventional three phase motor drives to multiphase motor drives [4]–[12]. FCS-MPC can be mainly classified into the following groups: Predictive current control (FCS-PCC) [4], [9], [10], predictive torque control (FCS-PTC) [5]–[8], predictive speed control (FCS-PSC) [11], [12].

It is desirable that the model used for the prediction is accurate enough. However, parameter mismatches and model uncertainties commonly exist in practice. The control performances are deteriorated under such unideal situations. The challenges of parameter mismatches and model uncertainties to MPC have gained increasing attention from the academic society. Recent works on the improvement of robustness for MPC are mostly implemented with *disturbance observers* [13]–[17]. In [13], disturbance observer (DOB)-based predictive torque control of induction motor has been proposed. In the speed loop, load DOB has been used to estimate the lumped disturbance, with which faster torque reference can be generated. In the inner loop, stator flux and torque observers are used. The system presents an improved robustness against the mechanical and electrical parameter uncertainties. In [14], DOB has been used to compensate the disturbance in the speed loop. Simplified stator flux observer is designed and stator resistance is estimated. In [15], incremental prediction model has been used to eliminate the effect of inaccurate rotor flux linkage. An inductance DOB has been used and the inductance is updated online. In [16] and [17], sliding mode observers are introduced to improve the robustness of the predictive current controller based on Dead-Beat (DB) concept. Disturbances are observed by the sliding mode observer. The estimated disturbances act as feed forward compensation voltage. The voltages applied to the inverters should be explicitly known in the DB-based MPC. It should be acknowledged that the sensitivity of MPC to mismatched models is decreased through the introduction of DOBs. However, the implementation of observers results

Manuscript received November 28, 2019; revised January 30, 2020; accepted March 7, 2020. Date of publication March 15, 2020; date of current version June 23, 2020. This work was supported by the National Key Research and Development Program of China under Grant 2018YFB0606001. Recommended for publication by Associate Editor R. Kennel. *(Corresponding author: Jin Wang.)*

Xicai Liu, Libing Zhou, Jin Wang, and Zhixiong Li are with the State Key Laboratory of Advanced Electromagnetic Engineering and Technology, School of Electrical and Electronic Engineering, Huazhong University of Science and Technology, Wuhan 430074, China (e-mail: xicai.liu@tum.de; zlb@mail.hust.edu.cn; hustwj@126.com; hustlzx@hust.edu.cn).

Xiaonan Gao is with the Institute for Electrical Drive Systems and Power Electronics, Technical University of Munich, 80333 Munich, Germany (e-mail: xiaonan.gao@tum.de).

Zhiwei Zhang is with the Department of Electrical and Computer Engineering, The Ohio State University, Columbus, OH 43210 USA (e-mail: zwzhangieee@gmail.com).

Color versions of one or more of the figures in this article are available online at http://ieeexplore.ieee.org.

Digital Object Identifier 10.1109/TPEL.2020.2980930

in higher computation burden and a more complicated control strategy.

Alternative solutions to improve the robustness of MPC without DOBs have been proposed in [18]–[23]. In [18] and [19], prediction error in the last sampling period has been used to improve the accuracy of the prediction. In [19], predictive current control is proposed, while predictive torque control has been proposed in [18]. Satisfactory results in terms of current/torque ripple reduction due to inductance mismatches are achieved. However, the influence of the mismatch in rotor flux linkage has not investigated with prediction error correction method. In [20], control-Lyapunov function (CLF)-based FCS-MPC control has been proposed. The stability of the proposed method is guaranteed through the selection of switching vectors which yield positive feedback gains. Adaptive compensation terms are estimated with the adaptive control law in integral form, which is used to compensate model uncertainties. It would be attractive that integral components could be incorporated into the cost function as an alternative to the design of adaptive law. It should be noted that integral term has been already included in publications [21]–[23]. In [21], FCS-MPC with integral action has been applied to a simple H-Bridge power converter to reduce the average steady-state error (SSE). The cost function is modified with the accumulated errors. Limited number of previous integral terms are included in the cost function in the implementation. In [22], explicit MPC (EMPC) with augmented model which considers the integral errors has been proposed for the control of induction motor fed by 3-level neutral point inverter. Offset-free steady-state performance at low switching frequency can be achieved. In [23], explicit model PCC with integral error feedback for doubly-fed induction generators has been proposed with an extended model. Analytical solution has been derived. Steady-state accuracy can be assured.

This article proposes a robust FCS-PCC strategy with a cost function in proportional-integral (PI) form for permanent-magnet synchronous motor (PMSM) drives, which is very simple and practical to implement. The accumulated errors are weighted with the sampling time and the integral action is activated in a predefined range. In this way, the design of the integral coefficients is facilitated. The main advantages of the proposed strategy can be listed as follows.

1) The proposed control strategy has the same control structure as the conventional PCC does. The only change is the modification of the conventional cost function. A new cost function in PI form is proposed to replace the conventional cost function.
2) Neither parameter identification nor DOB is introduced. SSEs due to inaccurate prediction under parameter mismatches are compensated by the integral term in the cost function.
3) No explicit solution needs to be derived compared to EMPC strategies. This article focuses on robust FCS-PCC without explicit solution, which is different from EMPC. In EMPC based on multiple-objective optimization, the compensation voltage provided by the integral term should be explicitly calculated.

This article is organized as follows. First, the model of PMSM considering parameter mismatches and model uncertainties is introduced. The nominal model for state variable prediction is given in discrete form. Second, the effects of parameter mismatches and possible improvement of the prediction by using prediction errors in the last sampling period is analyzed. Then, the proposed control strategy is given and its implementation is described in detail. Finally, the robustness of the proposed control strategy is validated through experiments.

II. System Description and Conventional PCC

In this section, mathematical model of 3-phase PMSM considering parameter mismatches and model uncertainties is derived and the basic principle of FCS-PCC for PMSM is briefly introduced.

A. Model of PMSM

The system dynamics of 3-phase PMSM considering parameter mismatches and model uncertainties in the synchronous rotating frame can be expressed as follows:

$$\frac{d}{dt}\mathbf{I}_{dq} = \mathbf{A}_c\mathbf{I}_{dq} + \mathbf{B}_c\mathbf{U}_{dq} + \mathbf{D}_c + \mathbf{F}_c \tag{1}$$

where

$$\mathbf{U}_{dq} = \begin{bmatrix} u_d(t) \\ u_q(t) \end{bmatrix}, \mathbf{I}_{dq} = \begin{bmatrix} i_d(t) \\ i_q(t) \end{bmatrix}$$

$$\mathbf{A}_c = \begin{bmatrix} -\frac{R_s}{L_d} & \frac{\omega_e(t)L_q}{L_d} \\ -\frac{\omega_e(t)L_d}{L_q} & -\frac{R_s}{L_q} \end{bmatrix}, \mathbf{B}_c = \begin{bmatrix} \frac{1}{L_d} & 0 \\ 0 & \frac{1}{L_q} \end{bmatrix}$$

$$\mathbf{D}_c = \begin{bmatrix} 0 \\ -\frac{\omega_e(t)\psi_f}{L_q} \end{bmatrix}, \mathbf{F}_c = \begin{bmatrix} f_d(t) \\ f_q(t) \end{bmatrix}$$

i_d and i_q are the d-axis and q-axis stator currents, respectively. u_d and u_q are the stator input voltages on the d-axis and q-axis, respectively. ω_e is the electrical angular speed of the rotor. L_d and L_q denote the nominal stator inductance on the d-axis and q-axis, respectively. ψ_f is the magnitude of the rotor flux linkage, R_s is the nominal stator resistance. f_d and f_q represent the lumped model uncertainties on the d-axis and q-axis, respectively, which are not explicitly given since the proposed control strategy considers them as lumped disturbances.

The discretization of (1) with a sampling period of T_s by using the one-step forward-Euler method yields

$$\mathbf{I}_{dq}(k+1) = \mathbf{A}_d(k)\mathbf{I}_{dq}(k) + \mathbf{B}_d(k)\mathbf{U}_{dq}(k) + \mathbf{D}_d(k) + \mathbf{F}_d(k) \tag{2}$$

where

$$\mathbf{U}_{dq}(k) = \begin{bmatrix} u_d(k) \\ u_q(k) \end{bmatrix}, \mathbf{I}_{dq}(k) = \begin{bmatrix} i_d(k) \\ i_q(k) \end{bmatrix}$$

$$\mathbf{A}_d(k) = \begin{bmatrix} 1 - \frac{R_sT_s}{L_d} & \frac{T_s\omega_e(k)L_q}{L_d} \\ -\frac{T_s\omega_e(k)L_d}{L_q} & 1 - \frac{R_sT_s}{L_q} \end{bmatrix}$$

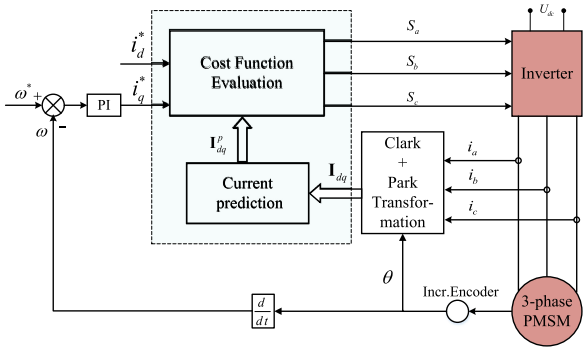

Fig. 1. Control diagram of Finite Control Set-PCC.

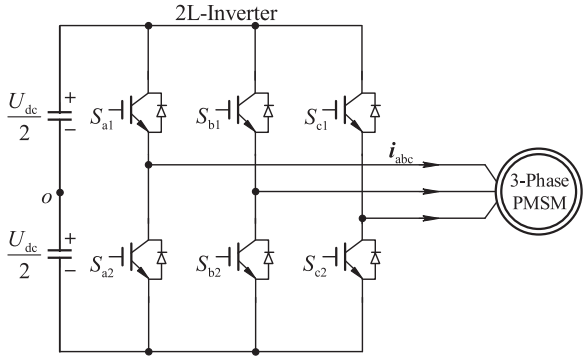

Fig. 2. 2-L voltage-source inverter.

$$\mathbf{B}_d(k) = \begin{bmatrix} \frac{T_s}{L_d} & 0 \\ 0 & \frac{T_s}{L_q} \end{bmatrix}, \mathbf{D}_d(k) = \begin{bmatrix} 0 \\ -\frac{T_s \omega_e(k) \psi_f}{L_q} \end{bmatrix}$$

$$\mathbf{F}_d(k) = \begin{bmatrix} f_d(k) \\ f_q(k) \end{bmatrix}.$$

B. Finite Control Set-PCC

Finite Control Set-PCC (FCS-PCC) for inverter-fed PMSM uses finite number of switching vectors to predict future value of stator currents with the model of PMSM. A cost function which defines the current tracking errors is designed for the implementation of the FCS-PCC. The cost function is evaluated for each of the admissible switching vectors and the switching vector which minimizes the cost function is applied to the inverter. The block diagram of FCS-PCC of PMSM is shown in Fig. 1.

Generally, f_d and f_q are neglected in conventional FCS-PCC. Otherwise, they should be estimated or compensated using DOBs or disturbance rejection methods. For each of the admissible candidate voltage vector $\mathbf{U}_{dq,admi}(k)$, one-step ahead prediction of the currents using the discrete nominal model of the motor yields

$$\mathbf{I}^p_{dq}(k+1) = \mathbf{A}_d(k)\mathbf{I}_{dq}(k) + \mathbf{B}_d(k)\mathbf{U}_{dq,admi}(k) + \mathbf{D}_d(k) \tag{3}$$

where

$$\mathbf{I}^p_{dq}(k+1) = \begin{bmatrix} i^p_d(k+1) \\ i^p_q(k+1) \end{bmatrix}.$$

The PMSM in this research is fed by 2-Level inverter (see Fig. 2), which means 8 admissible voltage vectors are possible

$$\mathbf{U}_{dq,admi}(k) = \mathbf{PCG} \tag{4}$$

where

$$\mathbf{C} = \frac{2}{3}U_{dc}\begin{bmatrix} 1 & -\frac{1}{2} & -\frac{1}{2} \\ 0 & \frac{\sqrt{3}}{2} & -\frac{\sqrt{3}}{2} \end{bmatrix}$$

$$\mathbf{P} = \begin{bmatrix} \cos(\theta_e) & \sin(\theta_e) \\ -\sin(\theta_e) & \cos(\theta_e) \end{bmatrix}, \mathbf{G} = \begin{bmatrix} g_a & g_b & g_b \end{bmatrix}^T$$

$\mathbf{G}$ represents the gate signals for the inverter

$$\mathbf{G} \in \Gamma_8 := \{000, 001, \ldots, 110, 111\}.$$

U_{dc} is the DC-link voltage and θ_e is the electrical angle of rotor.

For conventional PCC with one-step ahead prediction, the control objective is that the current tracking errors in the next sampling point become as small as possible. With this control goal, the cost function in the conventional PCC is designed as follows:

$$J = (e^p_d(k+1))^2 + (e^p_q(k+1))^2 \tag{5}$$

where

$$e^p_d(k+1) = i^*_d - i^p_d(k+1)$$
$$e^p_q(k+1) = i^*_q - i^p_q(k+1).$$

Since parameter mismatches and model uncertainties are not considered in the prediction model (3), prediction offset in the sampling interval $[(k-1)T_s \quad kT_s]$ is defined as the difference between the predicted currents $\mathbf{I}^p_{dq}(k)$ and actual sampled currents $\mathbf{I}_{dq}(k)$

$$\Delta^p_{dq}(k-1) = \mathbf{I}_{dq}(k) - \mathbf{I}^p_{dq}(k) = \mathbf{F}_d(k-1) \tag{6}$$

where $\mathbf{F}_d(k-1) = [f_d(k-1) \quad f_q(k-1)]^T$.

A small enough sampling time T_s yields

$$\Delta^p_{dq}(k-1) = \Delta^p_{dq}(k). \tag{7}$$

Obviously, the neglect of the unknown disturbances results in errors in the prediction, which will influence the selection of the optimal switching vector. SSEs will be more or less observed and the system may be unstable.

Remark 1: For PCC without constraints, the optimal solution of applied voltage is selected that the currents at the next sampling point $(k+1)$ are equal to the reference currents at the sampling instant k, i.e., $\mathbf{I}_{dq}(k+1) = \mathbf{I}^*_{dq}(k)$. An optimal applied voltage can be calculated with the parameters used in the prediction model

$$\mathbf{U}^*_{dq}(k) = \widehat{\mathbf{L}}_d(\mathbf{I}^*_{dq}(k) - \widehat{\mathbf{A}}_d(k)I_{dq}(k) - \widehat{\mathbf{D}}_d(k)) \tag{8}$$

where

$$\hat{\mathbf{L}}_d = \begin{bmatrix} \frac{\hat{L}_d}{T_s} & 0 \\ 0 & \frac{\hat{L}_q}{T_s} \end{bmatrix}, \hat{\mathbf{A}}_d(k) = \begin{bmatrix} 1 - \frac{\hat{R}_s T_s}{\hat{L}_d} & \frac{T_s \omega_e(k) \hat{L}_q}{\hat{L}_d} \\ -\frac{T_s \omega_e(k) \hat{L}_d}{\hat{L}_q} & 1 - \frac{\hat{R}_s T_s}{\hat{L}_q} \end{bmatrix}$$

$$\hat{\mathbf{D}}_d(k) = \begin{bmatrix} 0 \\ -\frac{T_s \omega_e(k) \hat{\psi}_f}{\hat{L}_q} \end{bmatrix}.$$

$\hat{R}_s, \hat{L}_d, \hat{L}_q$, and $\hat{\psi}_f$ are the actually known value of the stator resistance, $d-$axis inductance, $q-$axis inductance, rotor flux linkage, respectively. By substituting (8) into (2) and assuming a small enough sampling time, the closed-loop relationship transfer function can be obtained with the z transformation

$$\frac{I_d(z)}{I_d^*(z)} = \frac{\frac{\hat{L}_d}{L_{ds}}}{z - 1 + \frac{\hat{L}_d}{L_{ds}}} \tag{9}$$

$$\frac{I_q(z)}{I_q^*(z)} = \frac{\frac{\hat{L}_q}{L_{qs}}}{z - 1 + \frac{\hat{L}_q}{L_{qs}}} \tag{10}$$

where L_{ds} and L_{qs} represent the real value of the $d-$axis and $q-$axis inductance, respectively.

A discrete-control system is stable if all the eigenvalues are within the unit cycle. If no motor parameter-mismatches exist, the eigenvalues of the closed-loop system (9) and (10) are 0, which means the system is stable. However, in case of inductance error, the eigenvalues of the closed-loop system may be outside the unit cycle. FCS-PCC is a kind of predictive control with control constraints, where only finite number of switching states are feasible. The control of the currents in FCS-PCC is equivalent to the tracking of the optimal voltage [24]. The actual transfer function of the system deviates from (9) and (10) to some extent due to control constraints. Nonetheless, the pole placement of the system is parameter dependent, which means the stability of the control system is affected by parameter-mismatches.

To improve the accuracy of the prediction, $\mathbf{F}_d(k-1)$ is utilized in [18] and [19] to obtain corrected prediction

$$\hat{\mathbf{I}}_{dq}^p(k+1) = \mathbf{I}_{dq}^p(k+1) + \mathbf{K}\mathbf{F}_d(k-1) \tag{11}$$

where $\mathbf{K}$ is a diagonal gain matrix.

After the correction of prediction, the prediction offset in the sampling interval $[\ kT_s \quad (k+1)T_s\ ]$ becomes

$$\Delta_{dq}^p(k) = \mathbf{F}_d(k) - \mathbf{K}\mathbf{F}_d(k-1). \tag{12}$$

Prediction offset in (11) can be reduced through the incorporation of the correction term $\mathbf{K}\mathbf{F}_d(k-1)$ with appropriate gain matrix $\mathbf{K}$. However, prediction offset can not be fully eliminated with fixed gain matrix $\mathbf{K}$, as can be seen in (12). Moreover, a fixed gain matrix $\mathbf{K}$ is not optimal for all control conditions.

III. Proposed Control Strategy

A. Motivation

In conventional FCS-PCC, the evaluation of the cost function only considers the tracking errors between the reference currents and the predicted currents. As can be seen in (6), conventional FCS-PCC is highly parameter dependent and the robustness is low. To enhance the robustness, past tracking errors can be integrated into cost function, which means the cost function should be designed in PI form.

Stator current tracking errors in PI form can be expressed as S_d and S_q, which contains the present tracking error plus the integral of present as well as the past tracking errors are defined as

$$S_d = e_d(t) + K_d \int_0^t e_d(\tau) d\tau + e_d(0) \tag{13}$$

$$S_q = e_q(t) + K_q \int_0^t e_q(\tau) d\tau + e_q(0) \tag{14}$$

where $e_d(t) = i_d^* - i_d(t)$ and $e_q(t) = i_q^* - i_q(t)$ are the tracking errors of the stator currents on the d-axis and q -axis, respectively, K_d and K_q are positive gains. When the currents converge to the reference currents and steady-state is reached, following equations are valid

$$S_d = \frac{dS_d}{dt} = 0 \tag{15}$$

$$S_q = \frac{dS_q}{dt} = 0. \tag{16}$$

To implement FCS-MPC with integral action, S_d and S_q should be updated with the future tracking errors. In this way, the updated S_d and S_q, which includes previous tracking errors as well as future tracking errors are included in the cost function to evaluate the control performance of the proposed FCS-PCC. A cost function designed in PI form can force the future currents track the reference currents accurately with high robustness.

B. Proposed PCC Strategy

The proposed cost function can be designed in following steps:

1) Design of Draft Proportional-Integral Terms: In this step, draft PI terms are designed according to the (13) and (14). The main design task of this part is to design the gains K_d and K_q, which only considers the lumped disturbances. The convergence rates are not considered in this part. K_d and K_q can be selected with relatively small values since they are only designed to improve the robustness of the proposed control strategy.

Since FCS-PCC is implemented in discrete form, (13) and (14) are discretized in velocity form

$$S_d(k) = S_d(k-1) + (e_d(k) - e_d(k-1)) + K_d e_d(k) T_s \tag{17}$$

$$S_q(k) = S_q(k-1) + (e_q(k) - e_q(k-1)) + K_q e_q(k) T_s. \tag{18}$$

2) Incorporate the Draft Proportional-Integral Terms in the Cost Function: In this step, a cost function is designed by updating the discrete draft PI terms with the tracking errors between the predicted currents and reference currents

$$J = (S_d^p(k+1))^2 + (S_q^p(k+1))^2 \tag{19}$$

where

$$S_d^p(k+1) = S_d(k) + (e_d^p(k+1) - e_d(k)) + K_d e_d^p(k+1) T_s$$

$$S_q^p(k+1) = S_q(k) + (e_q^p(k+1) - e_q(k)) + K_q e_q^p(k+1) T_s.$$

A detailed analysis of the proposed cost function should be made to understand the robustness of the proposed algorithm. Since S_d^p is in the same form as S_q^p, only an analysis of S_d^p is given. The first component of $S_d^p(k+1)$ is the designed draft PI term $S_d(k)$, which contains the present current tracking error $e_d(k)$ and the integral of the tracking errors to time instant k. The integral action is essential for the robustness of the system since the information of lumped disturbances are contained in previous tracking errors. The inclusion of previous tracking errors in the cost function penalizes the voltage vector which can not compensate the previous SSEs. The second and third terms represent the equivalent tracking error between the reference current i_d^* and the predicted current $i_d^p(k+1)$, which forces the actual current i_d track the reference current as fast as possible. That is to say, the proposed control strategy inherits robustness from the integral action while quick response from the conventional FCS-MPC.

Remark 2: The proportional coefficients for S_d^p and S_q^p are set to 1, while the integral coefficients are designed as K_d and K_q, respectively. In this way, only the integral coefficients need to be tuned to meet the control goals, which facilitates the design of the cost function. FCS-MPC is a kind of control with high feedback control gains and the proportional coefficients in the proposed cost function are different from the actual feedback gains. The main issue which affects the control performance is the ratio between the proportional coefficients and the integral coefficients.

Remark 3: (Discussion on the robustness improvement): The proposed cost function (19) for different switching candidate states can also be expressed as

$$J = \left(i_d^* - i_d^p(k+1) + K_d T_s \sum_{j=1}^{k+1} e_d(j) \right) + \left(i_q^* - i_q^p(k+1) + K_q T_s \sum_{j=1}^{k+1} e_q(j) \right). \quad (20)$$

Let $\widetilde{f}_d(k)$ and $\widetilde{f}_q(k)$ defined as

$$\widetilde{f}_d(k) = \widetilde{i}_d^p - i_d^p(k+1) \quad (21)$$

$$\widetilde{f}_q(k) = \widetilde{i}_q^p - i_d^p(k+1) \quad (22)$$

where $\widetilde{i}_d^p$ and $\widetilde{i}_q^p$ are predicted currents on $d-$ and $q-$axis with a prediction model which exactly matches the actual system, respectively.

By substituting (21) and (22) into (20), the cost function can be expressed as

$$J = \left(i_d^* - \widetilde{i}_d^p + \widetilde{f}_d(k) + K_d T_s \sum_{j=1}^{k+1} e_d(j) \right) + \left(i_q^* - \widetilde{i}_q^p + \widetilde{f}_q(k) + K_q T_s \sum_{j=1}^{k+1} e_q(j) \right). \quad (23)$$

Each candidate switching vector results in corresponding values of $\widetilde{f}_d(k)$ and $\widetilde{f}_q(k)$. By designing the integral coefficients in a reasonable way, $\widetilde{f}_d(k)$ and $\widetilde{f}_q(k)$ can be used to compensate the accumulated errors by selecting a candidate switching vector which minimizes the cost function. In this way, the SSE will be gradually eliminated in receding-horizon manner. Equation (23) is used to illustrate how robustness can be improved while maintaining fast transient performance with the proposed cost function.

In reality, $\widetilde{f}_d(k)$, $\widetilde{f}_q(k)$ and $\widetilde{i}_d^p$ as well as $\widetilde{i}_q^p$ are unknown since an exactly matched model of the control system is out of reach. The cost function is evaluated to select the switching vector not in an analytical manner. The control performance is achieved through properly designed weighting factors.

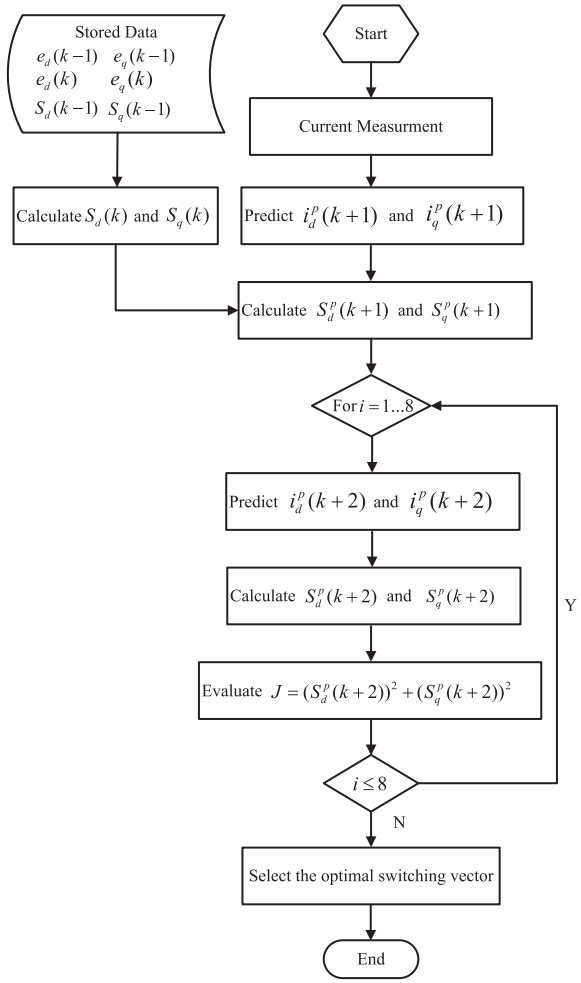

Fig. 3. Control flow of the proposed control strategy.

C. Implementation of the Proposed Strategy

In digital applications of FSC-MPC, computational delay should be considered. Normally, a one-step delay should be compensated. The implementation of the proposed strategy is shown in Fig. 3, which can be implemented as follows:

1) Apply the Selected Optimal Voltage of the Past Sampling Period: At time instant k the selected optimal voltage $\mathbf{U}_{dq,opt}(k-1)$ of the past sampling period $[\ (k-1)T_s \quad kT_s\ ]$

TABLE I
PMSM PARAMETERS

Parameter	Value
Nominal Stator Resistance [Ohm]	1.65
Nominal Stator Inductance [mH]	11.1
Nominal Rotor Flux Linkage ψ_f [Wb]	0.191
Rated line-to-line Voltage U_s^n [V]	116
Rated Current I^n [A]	4.95
Rated Torque T_e^n [Nm]	6
Rated Speed N_n [r/min]	1500
Motor Pole Pairs N_p [1]	3
Rotor Inertia J [Kgm^2]	8.7e-4

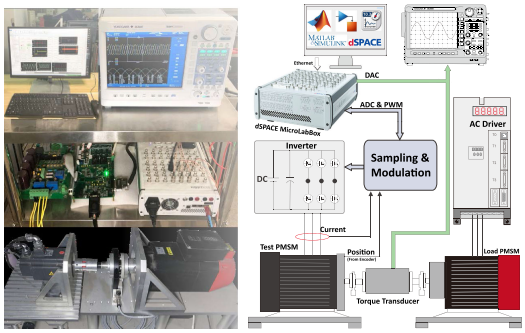

Fig. 4. Experimental setup.

is applied and the currents in the instant $k+1$ are predicted

$$\mathbf{I}_{dq}^{p}(k+1) = \mathbf{A}_d(k) I_{dq}(k) + \mathbf{B}_d(k)\mathbf{U}_{dq,opt}(k-1) + \mathbf{D}_d(k). \tag{24}$$

The predicted current tracking errors are expressed as

$$e_d^p(k+1) = i_d^* - i_d^p(k+1) \tag{25}$$

$$e_q^p(k+1) = i_q^* - i_q^p(k+1). \tag{26}$$

2) Update the Draft Proportional-Integral Terms With the Predicted Current Tracking Errors: The draft Proportional-Integral terms (17) and (18) are updated with (25) and (26), respectively

$$S_d^p(k+1) = S_d(k) + (e_d^p(k+1) - e_d(k)) + K_d e_d^p(k+1)T_s \tag{27}$$

$$S_q^p(k+1) = S_q(k) + (e_q^p(k+1) - e_q(k)) + K_q e_q^p(k+1)T_s. \tag{28}$$

To facilitate the design of integral coefficients, the integral parts in the cost function are activated only in predefined operation range. In this way, the coefficients K_d and K_q can be designed as

$$k_d = \begin{cases} 0, & abs((\omega_{ref} - \omega_r)/\omega_{ref}) > \varepsilon \\ k_{d,set}, & \text{else} \end{cases}$$
$$k_q = \begin{cases} 0, & abs((\omega_{ref} - \omega_r)/\omega_{ref}) > \varepsilon \\ k_{q,set}, & \text{else} \end{cases} \tag{29}$$

where ω_{ref} and ω_r are the reference value and actual value of the rotor speed, respectively. $k_{d,set}$ and $k_{q,set}$ are set values of K_d and K_q, respectively. ε represents the boundary of the predefined operation range in which the integral action activates.

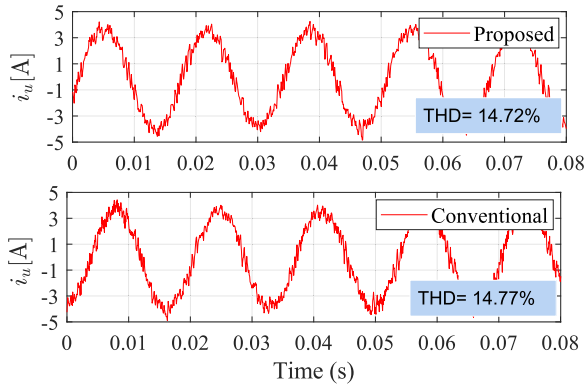

Fig. 5. [Experimental results: Stator phase current in nominal case]. Upper: Proposed method. Lower: Conventional method.

Remark 4: The integral action is only activated in a segmented manner since it is mainly used to improve the steady-state performance. With a well designed outer speed loop the actual speed will approach the defined range ε, even in case of some steady-state current tracking errors. The reason is that the $q-$axis current reference is adjusted by the outer-loop speed controller. As the integral action activates, the actual currents approach the reference currents eventually.

3) Incorporate the Updated Draft Proportional-Integral Terms in the Cost Function: First, the currents at instant $(k+2)$ are predicted with all the admissible voltages

$$\mathbf{I}_{dq}^{p}(k+2) = \mathbf{A}_d(k)\mathbf{I}_{dq}^{p}(k+1) + \mathbf{D}_d(k) + \mathbf{B}_d(k)\mathbf{U}_{dq,admi}(k+1). \tag{30}$$

Then, the updated draft PI terms (27) and (28) are incorporated in the cost function with the predicted current tracking errors

$$S_d^p(k+2) = S_d^p(k+1) + (e_d^p(k+2) - e_d^p(k+1)) + K_d e_d^p(k+2)T_s \tag{31}$$

$$S_q^p(k+2) = S_q^p(k+1) + (e_q^p(k+2) - e_q^p(k+1)) + K_q e_q^p(k+2)T_s. \tag{32}$$

The proposed cost function considering one-step delay can be expressed as

$$J = (S_d^p(k+2))^2 + (S_q^p(k+2))^2. \tag{33}$$

The cost function (33) is evaluated for each admissible voltage vector. The voltage vector $U_{dq,opt}(k)$ which minimizes the cost function is applied to the inverter at the sampling instant $k+1$.

Remark 5: In general, the cost function of the proposed method and the conventional method can be expressed in the same form (33) with different integral coefficients. For conventional method, $K_d = K_q = 0$.

IV. EXPERIMENTAL RESULTS

In this section, experimental results of the proposed robust PCC as well as the conventional PCC are presented and compared. A 3-phase surface-mounted PMSM has been used in this article. Nominal parameters of the motor are collected in Table I.

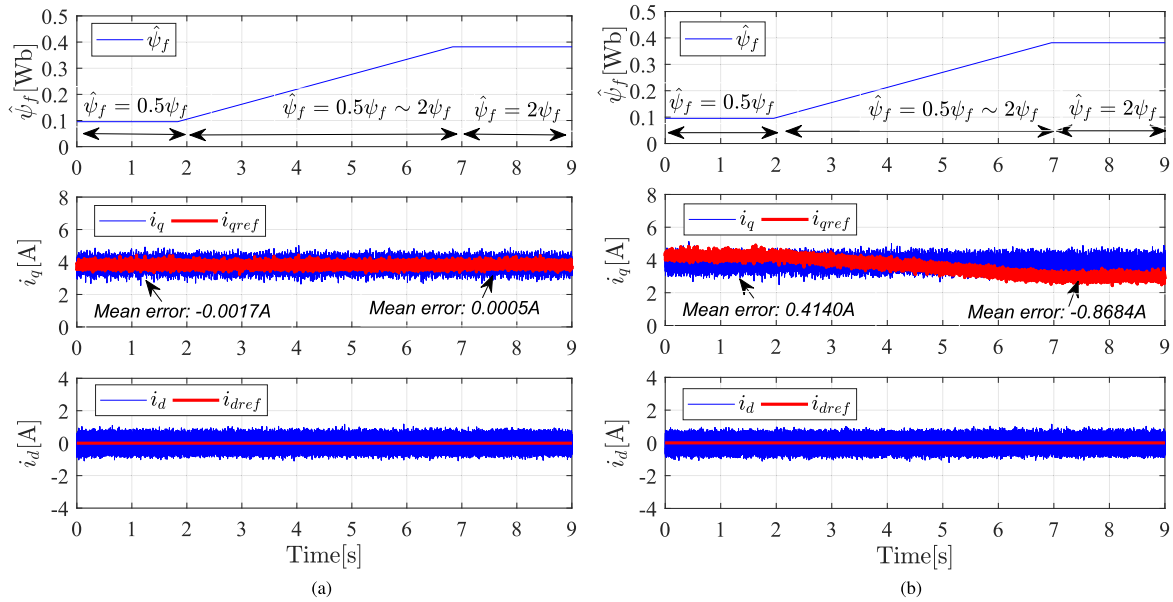

Fig. 6. [Experimental results: Robustness against rotor flux linkage mismatch]. (a) Proposed method. (b) Conventional method. From up to down are rotor flux linkage used in prediction model, $q-$ and $d-$axis current, respectively.

The test bench is shown in Fig. 4. A dSPACE MicrolabBox is employed as the controller. The dSPACE controller is connected to the power board through the interface board. The PMSM is coupled with a load machine, which is controlled by the load control unit. The load machine operates at torque mode. To obtain the steady-state results, the speed of the PMSM is controlled by outer speed loop with a PI controller, as shown in Fig. 1. The sampling frequency of the currents is 15 kHz for all the experimental tests. The DC-link Voltage U_{dc} is set to 295 V. For the proposed method, coefficients of integral terms are designed as $K_d = K_q = 10$ in the proposed cost function; The boundary for the activation of the integral action is set as $\varepsilon = 0.05$. For the conventional method, $K_d = K_q = 0$.

A. Robustness Evaluation of the Proposed Method and Conventional Method Against Parameter Mismatches

It should be mentioned that the influence of parameter mismatches in resistance is relatively small in PCC [19]. Thus, only uncertainties in inductance and rotor flux linkage are considered in following tests.

Comparison of the robustness of conventional PCC and proposed robust PCC are presented from Figs. 5 to 9. The motor rotates at 1200 r/min under a load torque of 2.9 Nm. Due to the existence of the outer speed loop, the mean magnitudes of the steady-state $q-$axis currents are the same. However, when the outer speed loop is removed, these magnitudes are different between the conventional method and the proposed method in case of parameter mismatches. In Fig. 5, no parameter mismatch exists, control performances of both methods are almost the same.

1) Rotor Flux Linkage Mismatch: When parameter mismatch occurs in rotor flux linkage, current tracking performance of the conventional method on $q-$axis deteriorates heavily. Obvious SSEs can be observed on $q-$axis for conventional method, while these tracking errors are eliminated for the proposed method. In Fig. 6, the value of the rotor flux linkage in the model is first set to $\hat{\psi}_f = 0.0955$ Wb, steady-state current tracking errors on $q-$axis with an average value of 0.4140 A [10.39% SSE] are obtained with conventional method. Then $\hat{\psi}_f$ increases from 0.0955 to 0.382 Wb. For $\hat{\psi}_f = 0.382$ Wb, average $q-$axis current tracking error of -0.8684 A (21.79% SSE) is observed with the conventional method. With error in rotor flux linkage, the back-EMF of the motor is inaccurately predicted. The current tracking errors of the conventional method depend on the speed of the motor and the error in the rotor flux linkage.

2) Stator Inductance Mismatch: When the value of the inductance $\hat{L}_s$ used in the prediction model is set to 5.55 mH (50% error in inductance), phase currents with both methods are distorted, which can be seen in Fig. 8. However, the phase currents are less distorted with the proposed method. The THD of the phase current is reduced from 15.96% for conventional method to 15.83% for proposed method. Negative current tracking errors (6.42% SSE) on $q-$axis can be observed with the conventional method, while these tracking errors are eliminated with the proposed method (see Fig. 7). When 100% error in inductance exists, large current ripples can be seen in both methods (see Fig. 9). With the proposed method, relatively less phase current ripples are presented. The THD of the phase current is 24.66% for conventional method and 22.27% for the proposed method. SSEs with an average value of 0.097 A on $d-$axis can be observed in Fig. 7 for the conventional method. Under 100% error in inductance, the average switching frequency f_{sw} is significantly lower for both methods in comparison to nominal case. Take the conventional method for example, average switching frequency decreases from 4075 Hz under nominal case to 3017 Hz under 100% error in inductance. The decrease of the average switching frequency exacerbates the phase current THD.

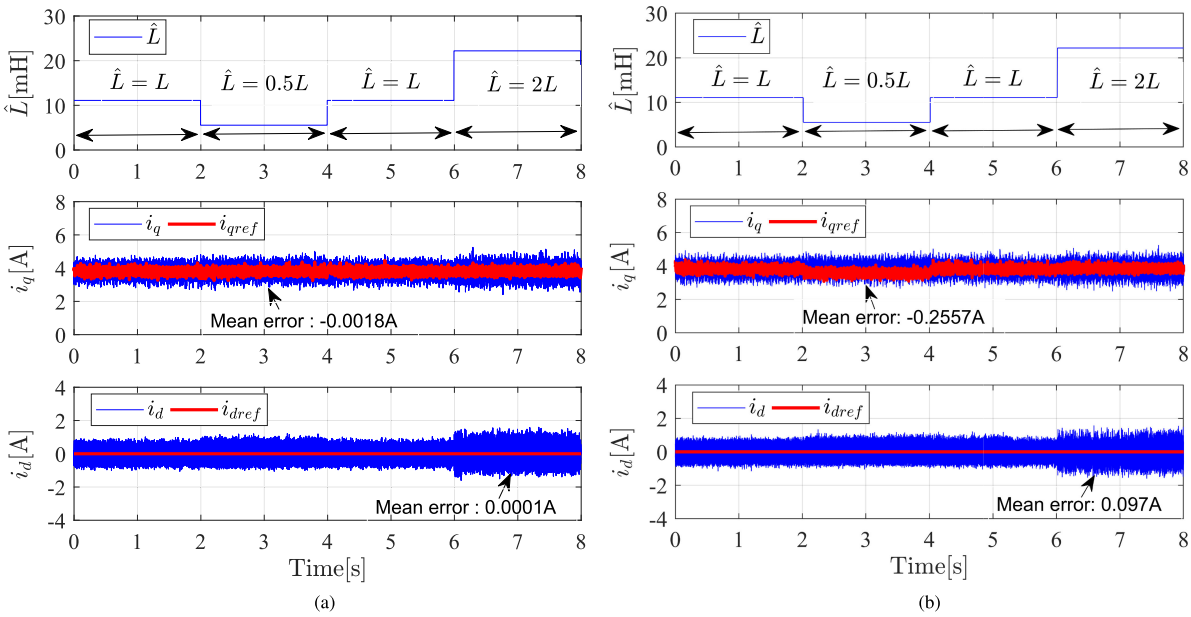

Fig. 7. [Experimental results: Robustness against stator inductance mismatch]. (a) Proposed method. (b) Conventional method. From up to down are stator inductance used in prediction model, $q-$ and $d-$axis current, respectively.

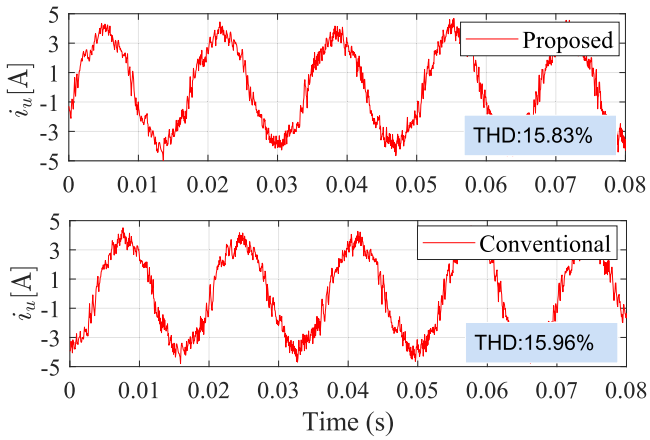

Fig. 8. [Experimental results: Stator phase current under 50% inductance error ($\hat{L}_s = 0.5L_s$). Upper: Proposed method. Lower: Conventional method.

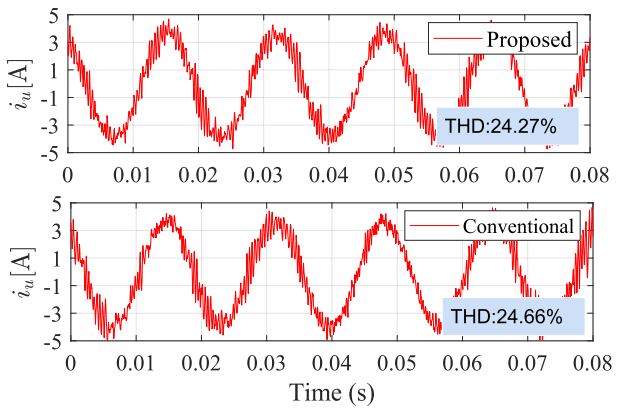

Fig. 9. [Experimental results: Stator phase current under 100% inductance error ($\hat{L}_s = 2L_s$). Upper: Proposed method. Lower: Conventional method.

B. Dynamic Performance Evaluation of the Proposed Method and Conventional Method in Case of Acceleration and Sudden Load Change

Dynamic responses of the proposed method and conventional method are also investigated. Only dynamic performances without parameter uncertainties are given due to page limits. Since the integral action only activates in predefined range, there is no need to provide all of the dynamics under various scenarios of parameter uncertainties. Accelerations of the motor from standstill to 1500 r/min at zero load torque are shown in Fig. 10. It can be seen that the proposed method exhibits a character of fast tracking performance as the conventional method, which can be explained with (29). The integral action of the proposed cost function is active only in a predefined range. The proposed method is the same as the conventional method as long as the integral action is not activated. The dynamic performance under sudden rated load torque of both methods is shown in Fig. 11. It can be seen that both methods have almost the same transient performance. This can be explained that under sudden load changes, the proportional part dominates and hence the dynamic performance is not affected. Prior to the application of the load torque, the reference currents can be well tracked with the proposed method and the value of the integral part is relatively small.

C. Summary

For conventional FCS-PCC, the actual currents deviate from the reference currents more or less in case of parameter mismatches, which can be seen from the experimental results. The reference current of the $q-$axis is given by the outer speed loop, which should provide a component to offset the SSE. In practice, the output of the PI speed controller has a limit value,

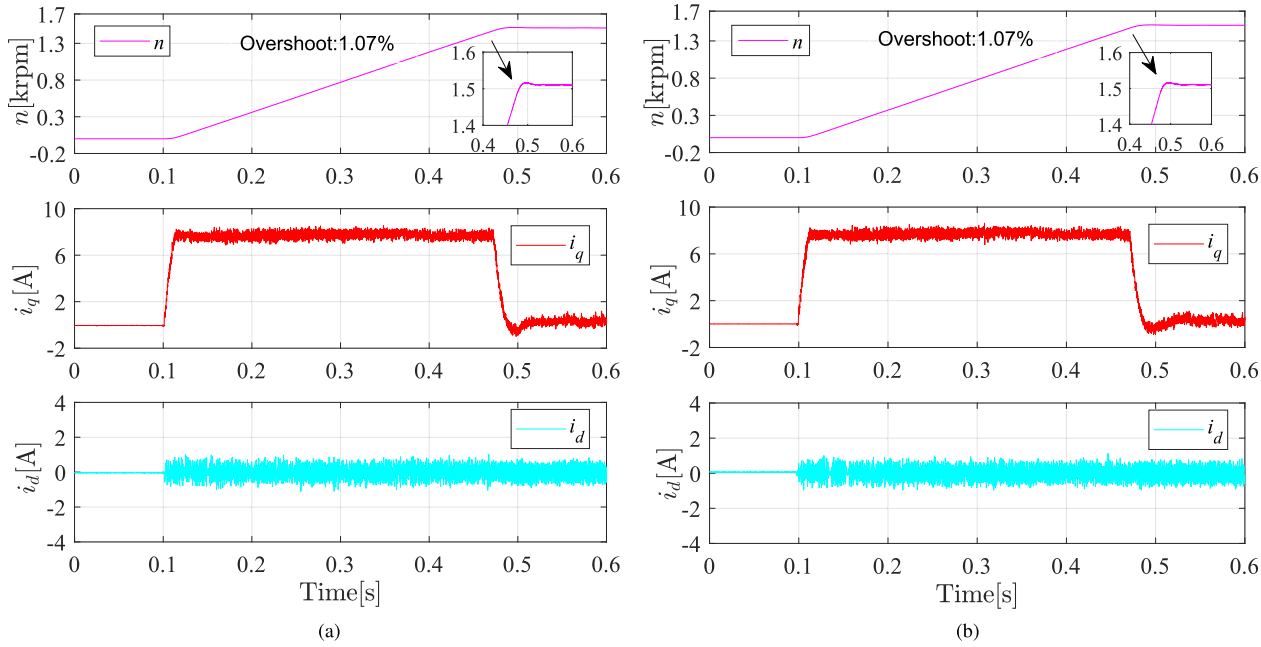

Fig. 10. [Experimental results: Dynamic performance from standstill to 1500 r/min without parameter mismatch]. (a) Proposed method. (b) Conventional method. From up to down are rotor speed, $q-$ and $d-$axis current, respectively.

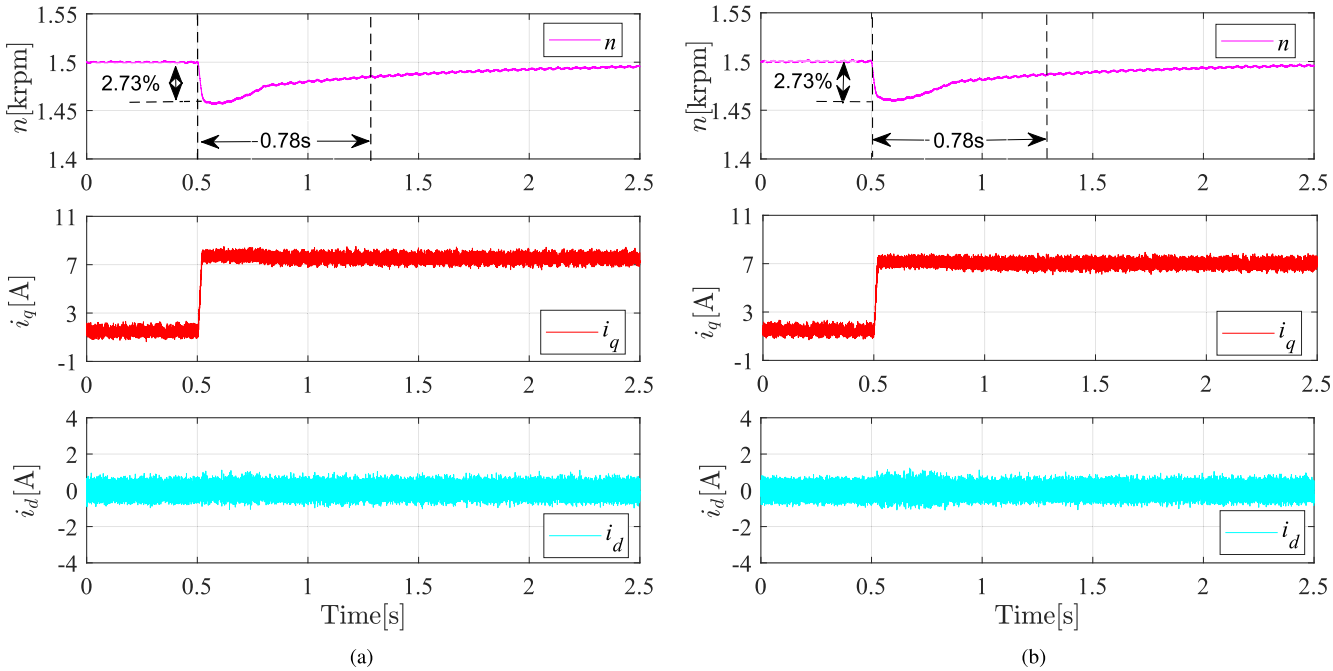

Fig. 11. [Experimental results: Dynamic performance in case of sudden rated load torque without parameter mismatch]. (a) Proposed method. (b) Conventional method. From up to down are rotor speed, $q-$ and $d-$axis current, respectively.

which is commonly used in the design of PI controller. When the output limit can't compensate the steady-state tracking error, the control system will face uncertainty. At full speed and full loaded, the output limit of the speed controller may not able compensate the SSE.

Steady-state performances of the conventional method and proposed method in terms of mean current tracking errors i_{qme} and i_{dme}, phase current THD as well as the average switching frequency f_{sw} are summarized in Tables II and III, respectively. i_{qme}, i_{dme} and f_{sw} are expressed as

$$i_{\text{qme}} = \frac{1}{N}\sum_{k=1}^{N}\left(i_q^*(k) - i_q(k)\right) \tag{34}$$

$$i_{dme} = \frac{1}{N}\sum_{k=1}^{N}\left(i_d^*(k) - i_d(k)\right) \tag{35}$$

$$f_{sw} = N_{sw}/Q/T \tag{36}$$

TABLE II
PERFORMANCE ANALYSIS OF CONVENTIONAL METHOD

Speed: 1200 rpm, Load Torque: 2.9 Nm

$\hat{L}_s$[mH]	$\hat{\psi}_f$[Wb]	i_{qme}[A]	i_{dme}[A]	f_{sw}[kHz]	THD(i_a)[%]
L_s	ψ_f	-0.0079	0.0309	4.0750	14.77
$0.5L_s$	ψ_f	-0.2557	-0.0257	4.1250	15.96
$2L_s$	ψ_f	0.0449	0.0970	3.0167	24.66
L_s	$0.5\psi_f$	0.4140	0.0344	3.9167	15.02
L_s	$2\psi_f$	-0.8684	-0.0222	3.8417	15.08

TABLE III
PERFORMANCE ANALYSIS OF PROPOSED METHOD

Speed: 1200 rpm, Load Torque: 2.9 Nm

$\hat{L}_s$[mH]	$\hat{\psi}_f$[Wb]	i_{qme}[A]	i_{dme}[A]	f_{sw}[kHz]	THD(i_a)[%]
L_s	ψ_f	0.0008	0.0001	3.9167	14.72
$0.5L_s$	ψ_f	-0.0018	-0.0004	3.8000	15.83
$2L_s$	ψ_f	0.0003	0.0001	3.3167	24.27
L_s	$0.5\psi_f$	-0.0017	0.0009	3.9667	14.90
L_s	$2\psi_f$	0.0005	-0.0008	3.9333	14.82

where N is the total sampling instants within the calculation period, T is the calculation period, N_{sw} is the number of switch operations within the calculation period, and Q is the number of inverter switches.

It should be noted that the aim of the proposed method is not the reduction of current ripples. The incorporation of the integral terms in the cost function mainly focuses on eliminating the SSEs. Nonetheless, the current ripples are slightly reduced and the phase currents are less distorted with the proposed method in case of inductance uncertainties.

V. CONCLUSION

In this article, a simple robust PCC strategy has been proposed. It has been shown that under parameter mismatches, inaccurate predictions affect the selection of optimal switching vector. SSEs can be observed with the conventional method. The main reason is that the cost function of conventional method only evaluates the tracking errors between the predicted currents and reference currents. To ensure the robustness against parameter mismatches, integral action which contains the information of parameter uncertainties has been included in the proposed cost function. The tuning of the integral coefficients in the proposed cost function is effortless. SSEs can be eliminated with the proposed method under parameter uncertainties while maintaining fast transient control performance. Moreover, less THD in phase currents is obtained with the proposed method compared to the conventional method in case of inductance uncertainties. Comparative experimental tests have been implemented and the effectiveness of the proposed robust control strategy has been validated under mismatched parameters.

APPENDIX

In this part, (9) and (10) are derived.

In the control of electrical drives, the sampling period of currents is generally very small. For a small enough sampling time T_s, it can be assumed that

$$\widehat{A}_d(k) = A_d(k) \approx \begin{bmatrix} 1 & 0 \\ 0 & 1 \end{bmatrix}.$$

By substituting the (8) into the equations of the motor, (2) can be expressed as

$$\begin{bmatrix} i_d(k+1) \\ i_q(k+1) \end{bmatrix} = \begin{bmatrix} i_d(k) \\ i_q(k) \end{bmatrix} + \begin{bmatrix} 0 \\ -\frac{T_s\omega_e(k)\psi_f}{L_{qs}} \end{bmatrix} + \begin{bmatrix} \frac{\widehat{L}_d}{L_{ds}} & 0 \\ 0 & \frac{\widehat{L}_q}{L_{qs}} \end{bmatrix} \left(\begin{bmatrix} i_d^*(k) \\ i_q^*(k) \end{bmatrix} - \begin{bmatrix} i_d(k) \\ i_q(k) \end{bmatrix} + \begin{bmatrix} 0 \\ \frac{T_s\omega_e(k)\widehat{\psi}_f}{\widehat{L}_q} \end{bmatrix} \right). \tag{37}$$

With the z transformation, (37) in z-domain is obtained as

$$\begin{bmatrix} (z - 1 + \frac{\widehat{L}_d}{L_{ds}})I_d(z) \\ (z - 1 + \frac{\widehat{L}_q}{L_{qs}})I_q(z) \end{bmatrix} = \begin{bmatrix} \frac{\widehat{L}_d}{L_{ds}} I_d^*(z) \\ \frac{\widehat{L}_q}{L_{qs}} I_q^*(z) \end{bmatrix}. \tag{38}$$

At this point, the deduce of (9) and (10) is done.

REFERENCES

[1] J. Rodriguez *et al.*, "State of the art of finite control set model predictive control in power electronics," *IEEE Trans. Ind. Inform.*, vol. 9, no. 2, pp. 1003–1016, May 2013.

[2] S. Vazquez, J. Rodriguez, M. Rivera, L. G. Franquelo, and M. Norambuena, "Model predictive control for power converters and drives: Advances and trends," *IEEE Trans. Ind. Electron.*, vol. 64, no. 2, pp. 935–947, Feb. 2017.

[3] S. Kouro, P. Cortes, R. Vargas, U. Ammann, and J. Rodriguez, "Model predictive control-a simple and powerful method to control power converters," *IEEE Trans. Ind. Electron.*, vol. 56, no. 6, pp. 1826–1838, Jun. 2009.

[4] Y. Zhang, D. Xu, J. Liu, S. Gao, and W. Xu, "Performance improvement of model-predictive current control of permanent magnet synchronous motor drives," *IEEE Trans. Industry Appl.*, vol. 53, no. 4, pp. 3683–3695, Jul. 2017.

[5] T. Geyer, G. Papafotiou, and M. Morari, "Model predictive direct torque control—part i: Concept, algorithm, and analysis," *IEEE Trans. Ind. Electron.*, vol. 56, no. 6, pp. 1894–1905, Jun. 2009.

[6] C. A. Rojas, J. Rodriguez, F. Villarroel, J. R. Espinoza, C. A. Silva, and M. Trincado, "Predictive torque and flux control without weighting factors," *IEEE Trans. Ind. Electron.*, vol. 60, no. 2, pp. 681–690, Feb. 2013.

[7] J. Rodriguez, R. M. Kennel, J. R. Espinoza, M. Trincado, C. A. Silva, and C. A. Rojas, "High-performance control strategies for electrical drives: An experimental assessment," *IEEE Trans. Ind. Electron.*, vol. 59, no. 2, pp. 812–820, Feb. 2012.

[8] J. A. Riveros, F. Barrero, E. Levi, M. J. Durán, S. Toral, and M. Jones, "Variable-speed five-phase induction motor drive based on predictive torque control," *IEEE Trans. Ind. Electron.*, vol. 60, no. 8, pp. 2957–2968, Aug. 2013.

[9] I. Gonzalez-Prieto, M. J. Duran, J. J. Aciego, C. Martin, and F. Barrero, "Model predictive control of six-phase induction motor drives using virtual voltage vectors," *IEEE Trans. Ind. Electron.*, vol. 65, no. 1, pp. 27–37, Jan. 2018.

[10] F. Wang, S. Li, X. Mei, W. Xie, J. Rodríguez, and R. M. Kennel, "Model-based predictive direct control strategies for electrical drives: An experimental evaluation of PTC and PCC methods," *IEEE Trans. Ind. Inform.*, vol. 11, no. 3, pp. 671–681, Jun. 2015.

[11] P. Kakosimos and H. Abu-Rub, "Predictive speed control with short prediction horizon for permanent magnet synchronous motor drives," *IEEE Trans. Power Electron.*, vol. 33, no. 3, pp. 2740–2750, Mar. 2018.

[12] X. Gao, M. Abdelrahem, C. M. Hackl, Z. Zhang, and R. Kennel, "Direct predictive speed control with a sliding manifold term for PMSM drives," *IEEE J. Emerg. Sel. Topics Power Electron.* early access, Jun. 17, 2019.

[13] J. Wang, F. Wang, Z. Zhang, S. Li, and J. Rodríguez, "Design and implementation of disturbance compensation-based enhanced robust finite control set predictive torque control for induction motor systems," *IEEE Trans. Ind. Inform.*, vol. 13, no. 5, pp. 2645–2656, Oct. 2017.

[14] L. Yan, M. Dou, Z. Hua, H. Zhang, and J. Yang, "Robustness improvement of fcs-mptc for induction machine drives using disturbance feedforward compensation technique," *IEEE Trans. Power Electron.*, vol. 34, no. 3, pp. 2874–2886, Mar. 2019.
[15] X. Zhang, L. Zhang, and Y. Zhang, "Model predictive current control for pmsm drives with parameter robustness improvement," *IEEE Trans. Power Electron.*, vol. 34, no. 2, pp. 1645–1657, Feb. 2019.
[16] B. Wang, Z. Dong, Y. Yu, G. Wang, and D. Xu, "Static-errorless deadbeat predictive current control using second-order sliding-mode disturbance observer for induction machine drives," *IEEE Trans. Power Electron.*, vol. 33, no. 3, pp. 2395–2403, Mar. 2018.
[17] Y. Jiang, W. Xu, C. Mu, and Y. Liu, "Improved deadbeat predictive current control combined sliding mode strategy for PMSM drive system," *IEEE Trans. Veh. Technol.*, vol. 67, no. 1, pp. 251–263, Jan. 2018.
[18] M. Siami, D. A. Khaburi, and J. Rodríguez, "Torque ripple reduction of predictive torque control for PMSM drives with parameter mismatch," *IEEE Trans. Power Electron.*, vol. 32, no. 9, pp. 7160–7168, Sep. 2017.
[19] M. Siami, D. A. Khaburi, A. Abbaszadeh, and J. Rodríguez, "Robustness improvement of predictive current control using prediction error correction for permanent-magnet synchronous machines," *IEEE Trans. Ind. Electron.*, vol. 63, no. 6, pp. 3458–3466, Jun. 2016.
[20] H. T. Nguyen and J. Jung, "Finite control set model predictive control to guarantee stability and robustness for surface-mounted PM synchronous motors," *IEEE Trans. Ind. Electron.*, vol. 65, no. 11, pp. 8510–8519, Nov. 2018.
[21] R. P. Aguilera, P. Lezana, and D. E. Quevedo, "Finite-control-set model predictive control with improved steady-state performance," *IEEE Trans. Ind. Inform.*, vol. 9, no. 2, pp. 658–667, May 2013.
[22] M. Jofré, A. M. Llor, and C. A. Silva, "Sensorless low switching frequency explicit model predictive control of induction machines fed by neutral point clamped inverter," *IEEE Trans. Ind. Electron.*, vol. 66, no. 12, pp. 9122–9128, Dec. 2019.
[23] C. Dirscherl and C. M. Hackl, "Model predictive current control with analytical solution and integral error feedback of doubly-fed induction generators with LC filter," in *Proc. IEEE Int. Symp. Predictive Control Elect. Drives Power Electron.*, Sep. 2017, pp. 25–30.
[24] L. Wang, S. Chai, D. Yoo, L. Gan, and K. Ng, *PID and Predictive Control of Electrical Drives and Power Converters Using MATLAB / Simulink*. New York, NY, USA: Wiley, 2015.

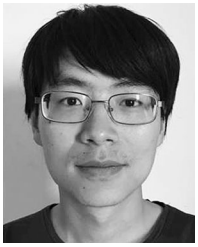

Xicai Liu received the double M.S. degree in control engineering from Tongji University, Shanghai, China and Technische Universitaet Muenchen Munich, Germany, in 2013. He is currently working toward the Ph.D. degree in electrical engineering from the Huazhong University of Science and Technology, Wuhan, China.

His major research interests include predictive control of electrical drives and power electronics.

Libing Zhou (Member, IEEE) received the B.S., M.S., and Ph.D. degrees from the Huazhong University of Science and Technology, Wuhan, China, in 1982, 1985, and 1993, respectively, all in electrical engineering.

He is currently a Professor with the Huazhong University of Science and Technology, Wuhan, China. His research interests include electromagnetic design, operation analysis, and drives of ac machines.

Jin Wang (Member, IEEE) received the B.S., M.S., and Ph.D. degrees from the Huazhong University of Science and Technology, Wuhan, China, in 2002, 2005, and 2010, respectively, all in electrical engineering.

From 2010 to 2013, he was a Postdoctoral Fellow with the Huazhong University of Science and Technology, where he is currently an Associate Professor. His research interests include electromagnetic design and analysis of permanent magnet machines and superconducting generators.

Xiaonan Gao (Student Member, IEEE) was born in Liaoning, China, in 1990. He received the B.S. and M.S. degrees in electrical engineering from the Dalian University of Technology, Dalian, China, in 2013 and 2016, respectively. He is currently working toward the Ph.D. degree with the Institute for Electrical Drive Systems and Power Electronics, Technical University of Munich, Germany.

His research interests include power electronics and electrical drives, predictive control, and multilevel converters.

Zhixiong Li (Student Member, IEEE) received the B.S. degree in electrical engineering and automation from China Three Gorges University, Yichang, China, in 2014. He is currently working toward the Ph.D. degree in electrical engineering with the Huazhong University of Science and Technology, Wuhan, China.

His major research interests include high performance permanent-magnet machine drives.

Zhiwei Zhang (Member, IEEE) received the Ph.D. degree in electrical engineering from the Huazhong University of Science and Technology, Wuhan, China, in 2016.

He is currently a Visiting Scholar with the Department of Electrical and Computer Engineering, The Ohio State University, Columbus, OH, USA. His current research interests include design and analysis of high-performance electric machines, variable-speed ac drives, transportation electrification, and renewable energy conversion systems.